Journal of Hazardous Materials 496 (2025) 139525

Contents lists available at ScienceDirect

Journal of Hazardous Materials

journal homepage: www.elsevier.com/locate/jhazmat

Foodborne metal(loid) contamination from coastal petrochemical industrial zone to countryside and urban zones: Spatial distribution and public health implications

Yanpeng Gao [a,b], Weixin Weng [a,b], Kai Huang [a,b], Shixing Ren [a,b], Richard W. Jordan [c], Shi-Jun Jiang [d], Yuemeng Ji [a,b], Yang-Guang Gu [e,*]

[a] Guangdong-Hong Kong-Macao Joint Laboratory for Contaminants Exposure and Health, Guangdong Key Laboratory of Environmental Catalysis and Health Risk Control, Guangdong Basic Research Center of Excellence for Ecological Security and Green Development, Institute of Environmental Health and Pollution Control, Guangdong University of Technology, Guangzhou 510006, China
[b] Guangzhou Key Laboratory of Environmental Catalysis and Pollution Control, Key Laboratory of City Cluster Environmental Safety and Green Development of the Ministry of Education, School of Environmental Science and Engineering, Guangdong University of Technology, Guangzhou 510006, China
[c] Faculty of Science, Yamagata University, Yamagata 990-8560, Japan
[d] State Key Laboratory of Marine Resource Utilization in South China Sea, Hainan University, Haikou, China
[e] South China Sea Fisheries Research Institute, Chinese Academy of Fishery Sciences, Guangzhou 510300, China

HIGHLIGHTS

- Application of the Double-Sample Food Method to assess metal(loid) pollution.
- Elevated As, Cd, and Pb concentrations in food from the coastal industrial zone.
- TTHQ and CR values indicate potential chronic and carcinogenic health risks.
- LLE and Random Forest reveal key contributors to pollutant distribution and risks.

GRAPHICAL ABSTRACT

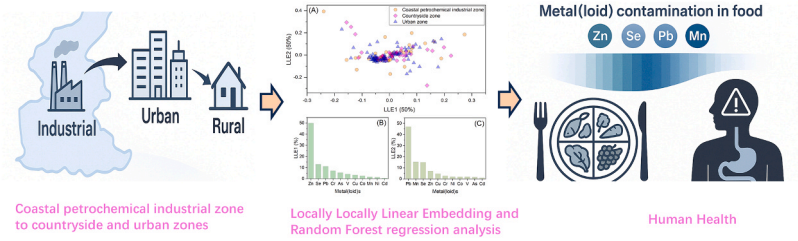

ARTICLE INFO

Keywords:
Metal(loid) contamination
Double-sample food method
Carcinogenic risk (CR)
Locally linear embedding (LLE)
Random forest regression

ABSTRACT

As industrialization and urbanization intensify in coastal regions, pollution from petrochemical zones can impact the metal(loid) content in food from nearby countryside and urban zones, posing public health risks. However, systematic assessments of the impact of coastal petrochemical activities on dietary metal(loid) exposure across countryside and urban populations remain limited. This study evaluated the spatial distribution and health risks of metal(loid) pollution along a land-use gradient—including a coastal petrochemical industrial zone, countryside, and urban zones. Food samples from the coastal petrochemical industrial zone showed elevated concentrations of toxic metal(loid)s, with As ranging from 2.40 to 5506.69 μg/kg, Cd from 1.07 to 4023.70 μg/kg, and Pb from 0.12 to 510.00 μg/kg—especially in seafood and leafy vegetables. The Total Target Hazard Quotient (TTHQ) often exceeded the safety threshold (TTHQ > 1), indicating potential chronic non-carcinogenic risks. Carcinogenic Risk (CR) values for arsenic were within or only slightly above the acceptable range (1×10^{-6} to 1×10^{-4}), suggesting possible long-term health threats. Locally Linear Embedding (LLE) combined with Random Forest regression suggests that coastal industrial activities are encroaching on neighboring areas and affecting the food of residents in non-industrial zones, and Zn, Se, Pb, and Mn emerge as the main drivers of the inter-zone

* Corresponding author.
E-mail address: hydrobio@163.com (Y.-G. Gu).

https://doi.org/10.1016/j.jhazmat.2025.139525
Received 31 May 2025; Received in revised form 24 July 2025; Accepted 9 August 2025
Available online 11 August 2025

differences and as the key metal(loid)s through which the coastal petrochemical industrial zone influences the environment.

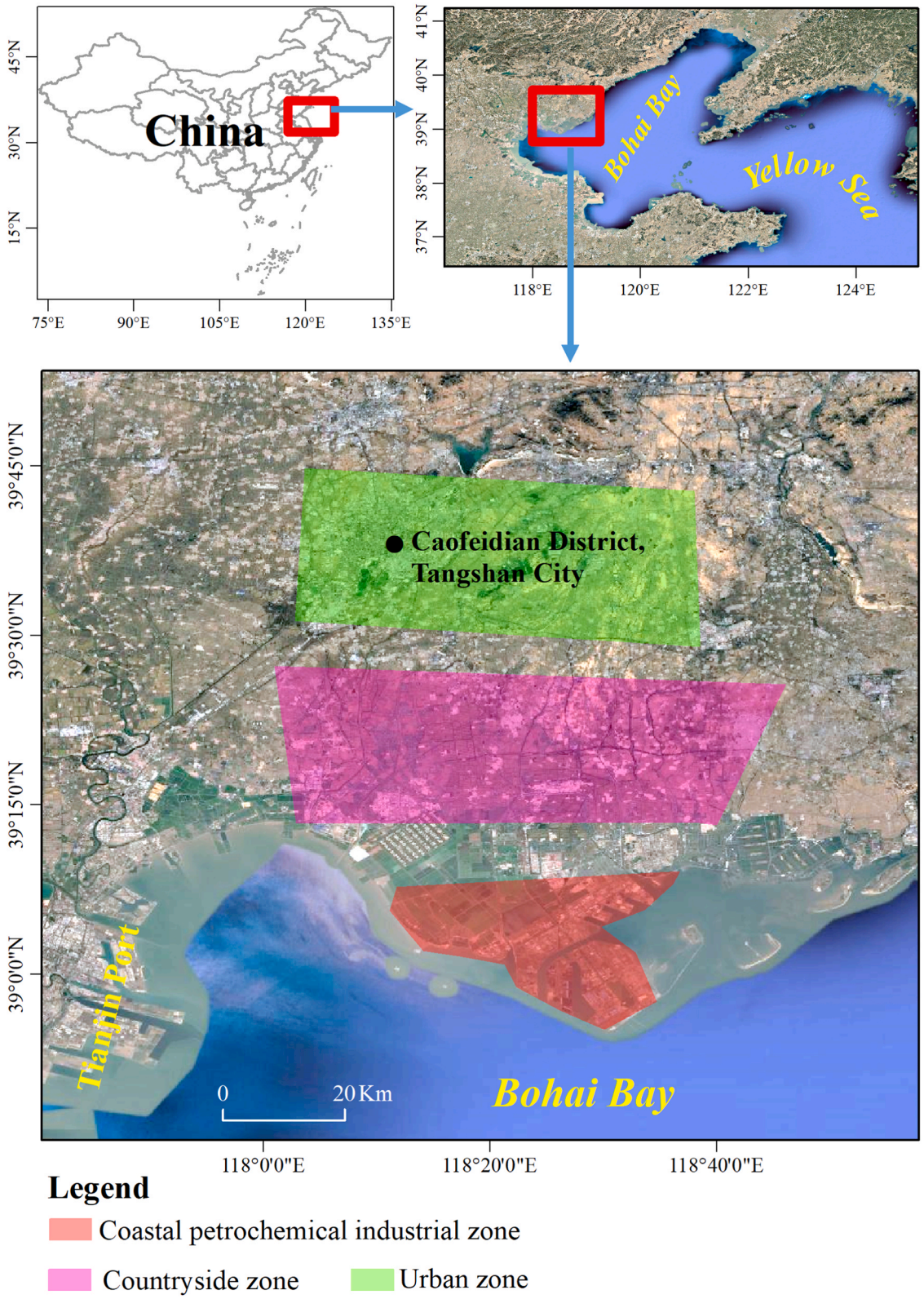

Fig. 1. Maps showing the study area, from a broad view to a detailed zoom-in, covering three zones in the Caofeidian District of Tangshan City, China.

1. Introduction

In recent years, the rapid development of industrialization and urbanization—especially in coastal regions—has led to escalating environmental pollution, particularly concerning metal(loid) contaminants and their potential threats to human health [1–4]. While previous research has extensively examined metal(loid) pollution in environmental media such as air, water, and soil, most studies focused on how contaminants from coastal industrial zones affect nearby countryside and urban zones through these media [5–9]. However, few studies explored how contaminants from industrial zones affect adjacent countryside and urban areas through food consumption—a direct and impactful exposure pathway. In such environments, atmospheric deposition (via gaseous emissions and particulate matter), contaminated irrigation water, and polluted soils may lead to the accumulation of metal(loid)s in crops and aquatic organisms. In this study, the sampled meals were prepared using vegetables, fish, and seafood primarily sourced from these impacted areas, thus reflecting real-world dietary exposure of local residents. Numerous studies have reported the occurrence of metal(loid) contamination in various foodstuffs, including vegetables, cereals, seafood, and animal products [10–16]. However, most of these studies have focused on individual food categories or specific contaminants, often neglecting systematic spatial assessments or comprehensive evaluations of total dietary exposure across different land-use zones. To address this gap, this study introduces a novel perspective by focusing on food as a critical medium for metal(loid) contamination and a key component of the "pollution-to-table" exposure route. It systematically investigates the levels and spatial distribution of metal(loid)s in food samples collected from three representative zones along an industrialization gradient: a coastal petrochemical industrial zone, a countryside zone, and an urban zone (Fig. 1).

To accurately capture the dietary exposure of local residents, this research employs the Double-Sample Food Method, a scientifically recognized and reliable approach that systematically collects food samples based on what residents actually eat and how much they consume in different zones. This method incorporates both dietary structure and intake levels, providing a more realistic and representative assessment of human exposure than conventional food sampling approaches that do not account for actual consumption patterns [17–19]. Moreover, advanced data analysis techniques, including Locally Linear Embedding (LLE) and Random Forest regression, are employed to reduce data dimensionality, explore spatial patterns, and assess the significance of individual metal(loid)s in shaping pollution profiles.

Non-metric Multidimensional Scaling (NMDS) is one of the most widely used non-linear dimensionality reduction methods in environmental and ecological studies, particularly for analyzing complex datasets such as metal(loid) contamination [4,6,20,21]. Locally Linear Embedding (LLE), originally proposed by Roweis and Saul in 2000 and published in *Science*, is another non-linear dimensionality reduction technique that offers distinct advantages in this context [22]. Though less commonly applied in environmental research, LLE preserves local geometric relationships, making it especially effective for capturing region-specific diffusion and propagation patterns of pollutants across industrial, countryside, and urban zones. In contrast, NMDS focuses on preserving global structures and relative distances between data points, which may overlook localized spatial patterns that are critical in environmental studies. Given this study's focus on localized pollution dynamics, LLE proves more effective than NMDS in revealing the nuanced, non-linear spatial relationships between pollutants and their sources. Therefore, LLE is adopted as the preferred dimensionality reduction method in this study.

To further interpret the results of LLE, Random Forest regression is applied to quantify the relative contribution of each individual metal (loid) to the variance explained by the two reduced dimensions (LLE1 and LLE2). This approach allows for identifying which metal(loid)s most strongly influence the spatial separation of samples in the reduced-dimensional space, thereby shedding light on the dominant pollutants driving differentiation among industrial, countryside, and urban zones. Unlike traditional linear models, Random Forests are well-suited for capturing complex, non-linear relationships and provide robust estimates of variable importance, even in the presence of noise or inter-variable correlations [23–26].

By jointly applying LLE and Random Forest regression, this study conducts—for the first time—a spatially explicit analysis of how a coastal petrochemical industrial zone influences adjacent countryside and urban zones. This integrated approach enhances the depth and reliability of the analysis, providing a comprehensive understanding of metal(loid) pollution patterns in food and offering novel insights into the spatial spread and health implications of industrial contamination.

The significance of this study lies in its dual contribution to both environmental science and public health. Firstly, it provides crucial empirical evidence of foodborne metal(loid) contamination in proximity to coastal petrochemical industrial zones—an area that has been relatively underexplored. Secondly, through spatial analysis and assessment of variable importance, the study uncovers how pollutants from industrial zones are transmitted to surrounding countryside and urban areas, revealing the key influencing factors and exposure pathways. These insights are essential for informing pollution control strategies, public health interventions, and sustainable regional planning.

By addressing significant gaps in existing research, the findings clarify the spatial distribution and community-level impacts of metal (loid) pollution and provide a theoretical foundation for the development of targeted environmental health policies. It establishes a new benchmark for assessing pollutant distribution and dietary exposure, emphasizing the urgent need for integrated approaches to protect both ecosystems and human health.

2. Materials and methods

2.1. Study area and sample collection

The study area is located in the Caofeidian District, Tangshan City, Hebei Province, China. Caofeidian District spans 1408.1 km^2 and lies within a temperate, semi-humid region of the eastern monsoon zone, featuring a distinct continental monsoon climate. The southern part, home to a petroleum industrial zone and port, serves as the region's economic hub, housing industries such as Jidong Petroleum extraction, steel mills, power plants, and chemical factories. The central area is primarily agricultural, while the northern part contains the main town. As of the 2020 census, the town had a permanent population of 112,660, including a large industrial workforce and their families. In 2021, the region's total GDP reached 85.063 billion yuan (RMB), with the secondary sector contributing 47.304 billion yuan (55.6 %). Key industrial outputs included 16.149 million tons of pig iron, 17.665 million tons of crude steel, 15.828 million tons of finished steel products, 19.32 billion kWh of electricity, 1.206 million metric tons of crude oil, and 1.8484 billion cubic meters of natural gas.

The duplicate diet study involved collecting food samples that were actually consumed by the participants, after being cooked and processed, to analyze chemical contaminant levels based on their dietary intake. This method is ideal for assessing the exposure of specific populations to chemical contaminants. From September to December 2022, a total of 163 duplicate diet samples were gathered from three different zones (Fig. 1). This included 47 samples from the coastal petrochemical industrial zone (CPIZ), 44 samples from the countryside zone (CZ), and 72 samples from the urban zone (UZ). The figure illustrates the sampling points across these regions.

To accurately reflect real-world dietary exposure in each zone, food items were selected based on typical meals consumed locally. Specifically, meals collected from the coastal petrochemical industrial zone primarily consisted of employee canteen and nearby restaurant dishes, representing the diet of local industrial workers. Meals from the

countryside zone were prepared in randomly selected farming households, while urban zone samples included both home-cooked meals and restaurant foods regularly consumed by urban residents. Due to actual dietary differences, the same standardized dishes were not collected across the three zones. Instead, locally consumed food combinations—comprising cereals, vegetables, seafood, meat, and other animal products—were collected to represent the real diets of local populations (Tables S1-S3). The main food ingredients (vegetables, fish, seafood, cereals, meat, etc.) were primarily sourced from local farms, markets, and aquaculture operations within each zone (Tables S1-S3).

After cooking, all meals were collected using standardized sampling protocols, and potential contamination from cooking utensils (e.g., woks, pans, ladles) was considered minimal, as standard stainless-steel or iron cookware was commonly used across all zones. Similarly, spices were not regarded as significant contributors to metal(loid) content, as primary ingredients dominated the meals. Importantly, the duplicate diet approach focuses on assessing total metal(loid) intake from whole meals, inherently accounting for all potential sources within typical food preparation.

After collection, the samples were sealed in plastic food storage bags and stored at −20 °C until they could be processed. All samples were carefully collected, separated, prepared, and stored individually to prevent cross-contamination.

2.2. Sample analysis

To streamline sample processing, the thawed duplicate diet samples were homogenized using a blender and then freeze-dried at −45 °C. After freeze-drying, the samples were ground again in a blender to improve digestion efficiency. Sample preparation and analysis in this study followed the Chinese National Standard (GB 5009.268–2016). For each sample, 0.2 g was weighed, and 6 mL of HNO_3 (≥65 %) was added to a microwave digestion vessel. The samples were pre-digested on a hot plate at 60 °C for 1 h, then 2 mL of H_2O_2 (≥30 %) was added before microwave digestion (CEM Corporation, MARS6) was conducted.

The microwave digestion program included three stages: heating to 100 °C and holding for 15 min., then to 120 °C for another 15 min., and finally to 140 °C for 25 min., with each stage taking 20 min. to reach the set temperature. After digestion, the samples were placed on a hot plate at 120 °C for 1 h to evaporate the remaining acid. The digestion solution was then diluted to 50 mL and filtered through a 0.45 μm filter for analysis. Concentrations of eleven metal(loid)s (V, Cr, Mn, Co, Ni, Cu, Zn, As, Se, Cd, Pb) were determined using inductively coupled plasma mass spectrometry (ICP-MS, Agilent 7500, USA).

2.3. Quality assurance and quality control

During sample collection and preparation, all food storage bags were exclusively used for sample collection to prevent any contamination. Containers used in the freeze-drying process were new 50 mL centrifuge tubes to avoid cross-contamination. Glassware used for homogenization and grinding was thoroughly cleaned before each use: initially with dishwashing detergent to remove grease, followed by multiple rinses with tap water, and finally rinsed three times with ultrapure water. For sample digestion, the digestion vessels were soaked in a 10 % HNO_3 solution for more than 24 h before use to ensure that all metal ions were completely removed. This process guarantees thorough removal of metal ions during digestion, enhancing the accuracy of the analysis.

To ensure the reliability of the experimental results, each batch included three ultrapure water blanks as controls to detect potential contamination. three mixed samples—composite homogenates prepared using equal portions of certified reference materials (GBW (E)100743 rice, GBW10231 spinach, and GBW10018 chicken)—and three gradient-spiked samples—matrix samples fortified at low (0.5 ×), medium (1 ×), and high (2 ×) expected concentration levels for each metal(loid)—were included in each batch to verify method accuracy. The deviation between the measured concentrations in the mixed samples and the certified values of the reference materials ranged from 85 % to 115 %, while spiked recovery rates ranged from 105 % to 108 %, confirming acceptable method accuracy. Laboratory blanks and duplicate samples were analyzed to assess method precision, with all relative standard deviations (RSDs) falling within the acceptable uncertainty range defined by national standards (i.e., the absolute difference between independent measurements under repeatability conditions did not exceed 10 % of the arithmetic mean). These combined quality control measures confirmed both the accuracy and precision of the analytical results.

2.4. Human health risk approach

2.4.1. Non-carcinogenic health risk approach

In this study, the non-carcinogenic health risk related to the consumption of food items from the three zones was evaluated using the target hazard quotient (THQ). The THQ is computed using the following Eq. (1) [27,28]:

$$THQ = \frac{EF \times ED \times FIR \times C}{RfD \times BW \times AT} \times 10^{-6} \quad (1)$$

Where EF represents the exposure frequency (days/year); ED is the exposure duration (years); FIR is the food ingestion rate (g/person/day); C represents the concentration of the metal(loid) in the food item (μg/kg); RfD represents the oral reference dose (g/day); BW represents the average body weight (kg); and AT represents average exposure time (days/year×ED). All parameters except for C are given in Table 1.

When individuals are exposed to multiple metal(loid)s, the combined health effects may be additive or interactive. Therefore, the total non-carcinogenic risk associated with a single food item is assessed by summing the THQ values of each individual element, as expressed in Eq. (2) [28]:

$$Total\ THQ(TTHQ) = \sum_i THQ_i \quad (2)$$

2.4.2. Carcinogenic health risk approach

According to the U.S. EPA classification, among the analyzed metal(loid)s in this study (V, Cr, Mn, Co, Ni, Cu, Zn, As, Se, Cd, and Pb), only arsenic (As) is classified as a carcinogenic element via the oral exposure

Table 1
Parameter settings and values adopted for the THQ estimation.

Parameter	Definition	Unit	Value	Reference
EF	exposure frequency	days/year	365	[28]
ED	exposure duration	years	77.87	[30]
FIR	food ingestion rate	g/person/day	1793.29	[31]
RfD	oral reference dose	mg/kg/day	5.0E−03 (V) 1.5E+ 00 (Cr)* 1.4E−01 (Mn) 3.0E−04 (Co) 2.0E−02 (Ni) 4.0E−02 (Cu) 3.0E−01 (Zn) 3.0E−04 (As) 5.0E−03 (Se) 1.0E−04 (Cd) 2.0E−02 (Pb)	[28,29]
BW	average body weight	kg	64.3	[32]
AT	average exposure time	days	365 × 70 = 25,550	[28]

* RfD value of Cr^{3+}used here. According to the U.S. EPA, only the RfD for tCr^{3+} is available. Additionally, based on previous studies, Cr in food items predominantly exists in the trivalent form [33–36]. Therefore, the RfD value of Cr^{3+} was used for health risk assessment in this study.

route. Therefore, carcinogenic risk assessment was conducted solely for As. The carcinogenic risk (CR) associated with the ingestion of food items contaminated with As is estimated using Eq. (3) [28]:

$$CR = \frac{EF \times ED \times FIR \times C \times CSF}{BW \times AT} \times 10^{-6} \quad (3)$$

Where CSF represents the oral carcinogenic slope factor, which was 1.5 (mg/kg/day) for As [29].

2.5. Statistical analysis

2.5.1. Multiple comparison analysis

To compare the concentrations of metal(loid)s among the three zones, a Q–Q plot was first used to assess the normality of the data, and this analysis was conducted using Origin 2022 SR1 for Windows. The results indicated that the concentrations of all metal(loid)s in each zone did not follow a normal distribution (Fig. S1). Therefore, the non-parametric Kruskal–Wallis test was employed to evaluate overall differences among the three zones. When significant differences were detected, Dunn's post hoc test was further conducted for multiple pairwise comparisons. Both the Kruskal–Wallis test and Dunn's post hoc test were performed using R version 4.4.3 for Windows, with the combined use of the FSA, dplyr, ggplot2, PMCMRplus, and effsize packages.

2.5.2. Hierarchical clustering and heatmap visualization

To investigate the spatial heterogeneity of metal(loid) contamination and potential source associations across zones, hierarchical clustering analysis combined with heatmap visualization was conducted using the maximum concentrations of each element per zone. The data were first normalized using Z-score standardization to eliminate unit scale bias and ensure comparability across metal(loid)s. This standardization was performed using the StandardScaler function from the sklearn.preprocessing module in Python 3.13.3.

Bi-directional hierarchical clustering was applied to both rows (metal(loid)s) and columns (zones), using the Ward's linkage method and Euclidean distance metric to measure similarities. The results were visualized as a clustered heatmap using the clustermap () function from the Seaborn package, built on Matplotlib and Pandas. The heatmap's color gradient reflects the standardized concentrations, indicating contamination hotspots and element groupings indicative of shared pollution sources or co-contamination patterns.

2.5.3. LLE dimensionality reduction and Random Forest regression analysis

To identify the dominant patterns of metal(loid) distribution across the three zones and to evaluate the potential influence of the coastal petrochemical industrial zone on the countryside and urban zones, a combination of Locally Linear Embedding (LLE) and Random Forest regression was applied. LLE is a nonlinear dimensionality reduction technique that preserves local neighborhood structures while projecting high-dimensional data into a lower-dimensional space [22]. In this study, the metal(loid) concentration data were reduced to two dimensions, denoted as LLE1 and LLE2. To assess the amount of information retained in the reduced space, the variance of LLE1 and LLE2, and their respective contribution ratios were calculated using the following Eq. (4):

$$Contribution\ Ratio_i = \frac{Variance\ of\ LLE_i}{Total\ Variance\ of\ LLE} \times 100 \quad (4)$$

where i refers to the two main components, LLE1 and LLE2. A higher contribution ratio indicates a greater amount of preserved information in the corresponding dimension.

Subsequently, to determine the influence of individual metal(loid)s on the observed spatial patterns, Random Forest regression models were employed. Each metal(loid) concentration was used as an independent variable, and LLE1 and LLE2 were treated as separate dependent variables. The resulting feature importance scores revealed which elements most strongly contributed to the underlying distribution patterns, thereby allowing us to identify the specific metal(loid)s through which the coastal petrochemical industrial zone may be exerting an impact on the other two zones.

All analyses were conducted using Python 3.13.3, with the required packages installed, including pandas, matplotlib, and scikit-learn.

3. Results and discussion

3.1. Metal(loid) concentrations in food samples from three distinct zones

The metal(loid) concentrations of 163 duplicate diet samples were collected from three zones: 47 from the coastal petrochemical industrial zone, 44 from the countryside zone, and 72 from the urban zone. These concentrations are illustrated in Fig. 2 and Tables S1-S3. In the CPIZ, the metal(loid) concentrations (μg/kg, dry weight) as follows: V (1.15 – 202.08), Cr (20.48 – 882.25), Mn (237.04 – 26114.25), Co (2.72 – 102.05), Ni (4.26 – 4426.25), Cu (138.00 – 19870.83), Zn (1778.26 – 57554.86), As (2.40 – 5506.69), Se (5.68 – 2288.74), Cd (1.07 – 4023.70), and Pb (0.12 – 510.00), with means (± SD) of 21.78 ± 32.25, 264.31 ± 168.89, 7217.93 ± 5264.03, 27.10 ± 25.58, 287.79 ± 663.58, 2840.38 ± 2947.02, 17841.69 ± 12824.95, 325.27 ± 963.24, 261.96 ± 396.53, 113.08 ± 584.94, 33.12 ± 80.57, respectively (Fig. 2 and Table S1).

In CZ, the metal(loid) concentrations (μg/kg, dry weight) were: V (0.37 – 121.28), Cr (9.20 – 871.38), Mn (2009.25 – 46763.72), Co (0.48 – 88.41), Ni (0.63 – 570.68), Cu (861.07 – 27924.48), Zn (2911.22 – 60487.77), As (1.25 – 1367.37), Se (11.50 – 715.78), Cd (0.38 – 87.28), and Pb (0.75 – 271.57), with means (± SD) of 34.45 ± 36.50, 206.38 ± 174.40, 7792.64 ± 7214.25, 17.69 ± 15.81, 151.27 ± 156.15, 3271.24 ± 4448.78, 16710.62 ± 10942.45, 299.30 ± 369.46, 209.16 ± 195.93, 19.99 ± 20.68, 38.58 ± 58.87 (Fig. 2 and Table S2).

In UZ, the metal(loid) concentrations (μg/kg, dry weight) were: V (0.50 – 186.49), Cr (8.48 – 1333.33), Mn (569.38 – 30876.87), Co (1.98 – 88.51), Ni (1.62 – 1466.25), Cu (357.49 – 10324.83), Zn (2800.2 – 88258.5), As (1.25 – 1308.15), Se (2.02 – 1146.18), Cd (0.44 – 319.31), and Pb (0.12 – 276.42), with means (± SD) of 18.42 ± 24.07, 234.78 ± 209.36, 7580.69 ± 6889.33, 22.01 ± 18.14, 193.76 ± 243.95, 2490.54 ± 1687.12, 20087.64 ± 17094.5, 74.60 ± 185.14, 179.85 ± 238.22, 25.81 ± 45.63, 37.34 ± 49.13 (Fig. 2 and Table S3).

Kruskal-Wallis multiple comparison analysis of metal(loid) concentrations among the three study zones—CPIZ, CZ, and UZ—showed no significant differences ($p > 0.05$) for V, Cr, Mn, Co, Ni, Cu, Zn, Se, Cd, and Pb (Table 2). However, As and Pb exhibited significant spatial variation ($p < 0.05$) (Table 2). Subsequent Dunn's post hoc tests revealed that As concentrations in the CPIZ were significantly higher than those in both the urban and countryside zones (Table 2). Conversely, Pb concentrations were significantly elevated in the UZ and CZ compared to the CPIZ, with no significant difference between the urban and countryside zones (Table 2).

It should be noted that while the types of meals varied across zones—reflecting local dietary habits and food sourcing practices—efforts were made to minimize external contamination sources. All meals were prepared using locally sourced vegetables, seafood, and livestock products representative of each region's typical diet. Additionally, pre-cooked food samples were collected directly from households, employee canteens, and restaurants, thus reflecting actual dietary exposures. Since sampling occurred after food preparation, potential contamination from cooking utensils or spices could not be entirely excluded. However, given the diversity and large number of food items sampled within each zone, such influences are likely random rather than systematic, and therefore unlikely to bias inter-zone comparisons significantly. Nonetheless, this limitation should be considered when interpreting the observed spatial patterns. These spatial differences may be attributed to varying anthropogenic inputs and land-use

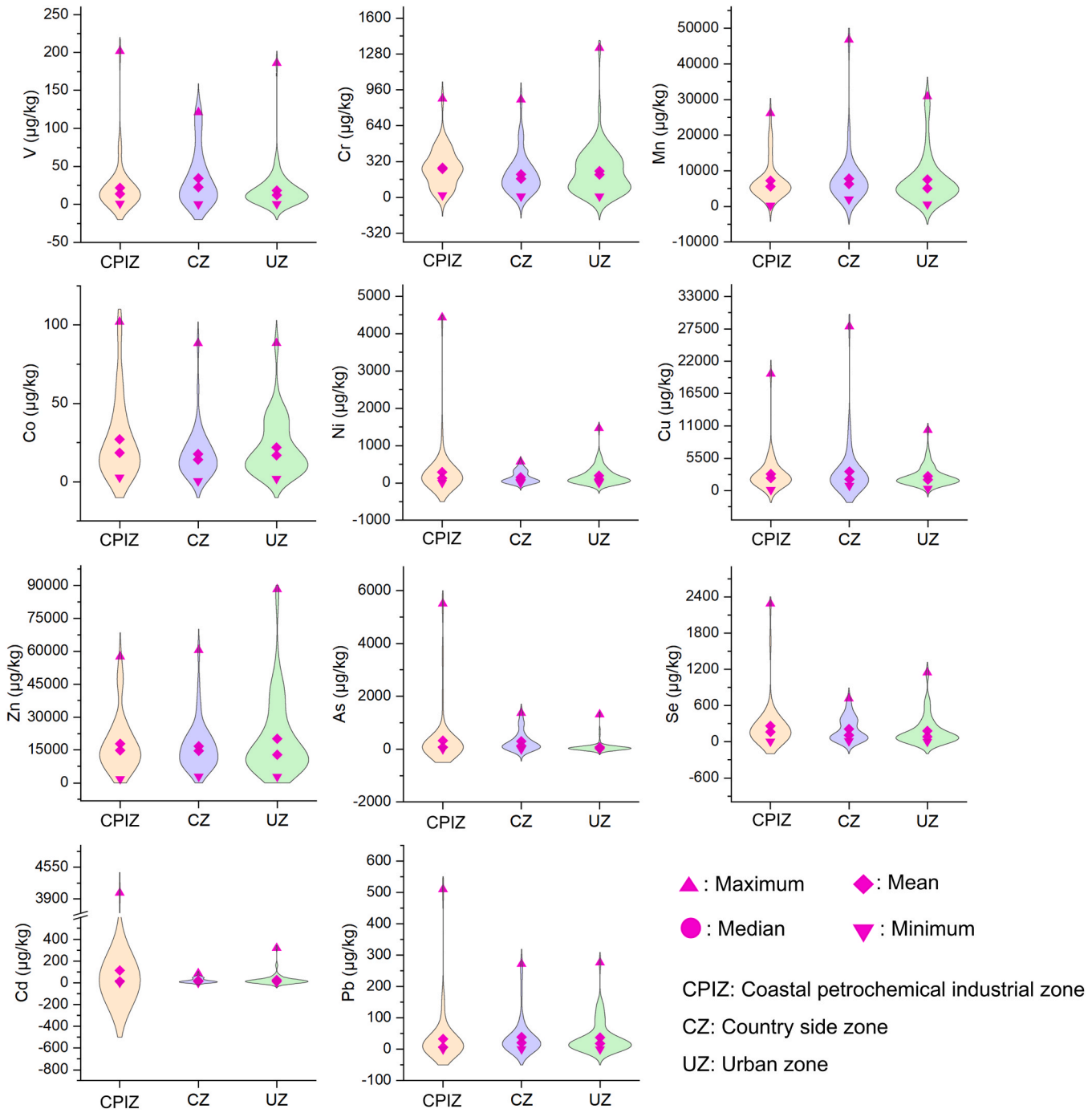

Fig. 2. Violin plots of metal and arsenic concentrations in food samples from three zones in the Caofeidian District of Tangshan City, China.

characteristics among the three zones. The elevated As levels in the CPIZ could be linked to emissions from industrial processes such as petroleum refining and chemical manufacturing. In contrast, higher Pb concentrations in the UZ and CZ may result from historical use of leaded gasoline, traffic emissions, and agricultural activities involving lead-based pesticides or fertilizers.

Compared to published data from other regions of China, the metal (loid) concentrations observed in this study were generally comparable to typical ranges, although certain concentrations were slightly elevated in some samples. For instance, As concentrations in CPIZ food items (up to 5506.69 μg/kg, dry weight) were comparable to or higher than previously reported levels in seafood from coastal or industrial regions [14, 37]. In contrast, vegetables cultivated near industrial or urban areas have generally been reported to contain lower arsenic concentrations [38,39]. These findings suggest that As accumulation in CPIZ food items reflects anthropogenic inputs at levels similar to or moderately above those observed in other regions. Similarly, Pb concentrations in UZ and CZ samples (up to 271.57 and 276.42 μg/kg, respectively) were broadly comparable to levels reported in large urban centers such as Shanghai and Beijing [12,39], indicating contributions from urban traffic, industrial emissions, and agricultural practices.

In contrast, metals showing no significant spatial differences (e.g., Cr, Cu, Zn, Se) likely reflect regionally consistent contamination patterns, possibly due to widespread agricultural inputs, diffuse industrial emissions, or shared food supply chains. Trace metals such as Mn and Ni, which also exhibited limited spatial variation, are generally controlled

Table 2
Kruskal-Wallis test and Dunn's comparison for metal(loid) concentrations in coastal petrochemical industrial zone (CPIZ), countryside zone (CZ), and urban zone (UZ).

Element	Kruskal-Wallis Chi-squared test	Degrees of freedom	*p*-value
V	4.17	2	1.24E−01
Cr	3.79	2	1.50E−01
Mn	0.84	2	6.57E−01
Co	2.65	2	2.65E−01
Ni	1.32	2	5.16E−01
Cu	0.14	2	9.32E−01
Zn	0.05	2	9.74E−01
As	32.52	2	8.69E−08
Se	5.04	2	8.07E−02
Cd	0.30	2	8.60E−01
Pb	7.15	2	2.81E−02
	Dunn's comparison	Z score	*p*-value
As	CPIZ vs. CZ	2.19	2.85E−02
	CPIZ vs. UZ	3.24	1.18E−03
	CZ vs. UZ	5.58	2.41E−08
Pb	CPIZ vs. CZ	2.33	1.97E−02
	CPIZ vs. UZ	2.36	1.83E−02
	CZ vs. UZ	0.24	8.07E−01

by natural geochemical backgrounds rather than localized anthropogenic sources.

Overall, although no significant inter-zone differences were observed for most metals, the spatial patterns of As and Pb highlight localized environmental contamination risks associated with industrial and urban activities. These findings are consistent with the observed spatial clustering and underscore the need for targeted risk management strategies focusing on arsenic and lead exposure. Furthermore, this regional dietary contamination assessment complements previous studies, reaffirming that coastal, industrial, and urban areas remain priority zones for the monitoring and control of metal(loid) contamination in food.

3.2. Metal(loid)s in different food items from three different zones

The concentrations of metal(loid)s in food items collected from the three study zones are summarized in Tables S1–S3. In the CPIZ, the highest concentration of V was observed in Sample ID CPIZ27 (rice, crab, and shrimp), reaching 202.08 μg/kg. Cr exhibited its peak value of 882.25 μg/kg in Sample ID CPIZ10, which contained oil-splashed noodles. Manganese (Mn) reached the highest concentration of 26,114.25 μg/kg in Sample ID CPIZ3 (tofu skin, liangpi, and yuba). The maximum cobalt (Co) level, 102.05 μg/kg, was detected in Sample ID CPIZ15, consisting of sweet potato. The greatest nickel (Ni) concentration, 4426.25 μg/kg, was found in Sample ID CPIZ16 (peanuts, wood ear mushrooms, and green peppers). Notably, Sample ID CPIZ27 also recorded the highest levels of copper (Cu, 19,870.83 μg/kg), arsenic (As, 5506.69 μg/kg), and cadmium (Cd, 4023.70 μg/kg). Zinc (Zn) reached its maximum at 57,554.86 μg/kg in Sample ID CPIZ8 (mushrooms and romaine lettuce), while selenium (Se) peaked at 2288.74 μg/kg in Sample ID CPIZ22 (steamed bun and sweet potato). Lead (Pb) was highest in Sample ID CPIZ14 (scrambled eggs with shredded potatoes), with a concentration of 510.00 μg/kg. Notably, the CPIZ zone exhibited the highest concentrations of As, Cd, Cu, Ni, and Pb across all samples, particularly in those containing seafood or leafy vegetables. This suggests a possible link between industrial emissions and the bioaccumulation of toxic metals in local food chains. Notably, many of these high-concentration samples contained seafood or leafy vegetables, both of which are recognized for their high metal accumulation capacity. The diversity of sampled dishes, reflective of local dietary habits, may partially explain the observed variations between food items. However, all samples were prepared using locally sourced ingredients representative of each zone's typical diet, minimizing the influence of external contamination sources. Furthermore, sampling after cooking inevitably introduced potential variability from utensils or spices, though these factors were randomized across the large sample pool and are unlikely to systematically bias zone-based comparisons. It is also acknowledged that differences in food types across zones may influence measured metal(loid) concentrations due to varying accumulation capacities among food categories. Thus, the present study's findings reflect the combined effects of environmental contamination and regional dietary structures. The elevated Cd and As levels in seafood-rich meals may pose significant health risks, especially due to the known carcinogenic and nephrotoxic effects of these elements.

In the CZ, the highest V concentration (121.28 μg/kg) was found in Sample ID CZ23 (rice and fish), while Cr peaked at 871.38 μg/kg in Sample ID CZ16 (rice and daikon radish). Mn exhibited a maximum concentration (46,763.72 μg/kg) in Sample ID CZ15 (wheat pancake, crab, and pork with cabbage). The highest Co content (88.41 μg/kg) occurred in Sample ID CZ20 (rice and stir-fried chicken with potatoes). Ni reached a peak of 570.68 μg/kg in Sample ID CZ23 (rice and fish). Cu was highest at 27,924.48 μg/kg in Sample ID CZ35 (rice and shrimp), and Zn reached 60,487.77 μg/kg in Sample ID CZ40 (rice, pork, and long beans). As peaked at 1367.37 μg/kg in Sample ID CZ7 (rice and fish), while Se was highest at 715.78 μg/kg in Sample ID CZ31 (rice and fish). Cd showed a maximum concentration (87.28 μg/kg) in Sample ID CZ5 (rice and peanuts), and Pb reached 271.51 μg/kg in Sample ID CZ27 (rice, chive and egg dumplings, and lettuce). Compared to CPIZ, the countryside zone displayed overall moderate metal(loid) levels, with occasional spikes in Cu and Mn concentrations. Rice- and fish-based combinations were common in samples with higher As and Se, indicating possible input from aquaculture or water sources. Cd and Pb concentrations remained significantly lower than in CPIZ, suggesting relatively lower anthropogenic impact in this zone. Nonetheless, occasional spikes in certain items, especially rice- and fish-based combinations, may reflect input from aquaculture water or agricultural practices specific to the countryside.

In the UZ, the highest concentration of V (186.49 μg/kg) was detected in Sample ID UZ58 (tofu, fish, and cabbage). Cr peaked at 1333.33 μg/kg in Sample ID UZ47 (duck meat). Mn showed a maximum value (30,876.87 μg/kg) in Sample ID UZ53 (greens and wood ear mushrooms), and Co was highest (88.51 μg/kg) in Sample ID UZ68 (pork, eggplant, chili, and wood ear mushrooms). Ni reached 1466.25 μg/kg in Sample ID UZ48 (bean sprouts and hot pot meatballs). Cu was again highest in UZ58 (10,324.83 μg/kg), while Zn peaked at 88,258.50 μg/kg in Sample ID UZ62 (winter melon rice and carrots). The highest value (1308.15 μg/kg) of As occurred in Sample ID UZ45 (winter melon), and Se peaked at 1146.18 μg/kg in Sample ID UZ8 (egg). Cd was most concentrated in Sample ID UZ60 (shiitake mushrooms and greens) at 319.31 μg/kg, while the highest level (276.42 μg/kg) of Pb occurred in Sample ID UZ2 (Ma La Gao and leafy greens). The urban zone showed high variability in metal concentrations, with Zn, Cr, and Cd levels occasionally exceeding those in the countryside. Zn in particular was markedly elevated in vegetable-based dishes, likely due to urban soil contamination or intensive vegetable farming. While the overall As and Pb levels were lower than CPIZ, the sporadic presence of high Cd in mushroom-based foods raises concerns about food-specific exposure risks. In particular, fungi are known bioaccumulators of heavy metals, which may explain some of the isolated high Cd levels detected in mushroom-containing dishes. Given the inherent differences in food categories among zones due to local eating habits, direct item-to-item comparison was not the focus; instead, the study prioritized assessing overall dietary exposure patterns within each representative zone.

The heatmap combined with hierarchical clustering analysis based on the maximum concentrations of metal(loid)s across the three zones reveals distinct spatial differentiation in contamination profiles, likely reflecting varying anthropogenic inputs and environmental conditions (Fig. 3). Notably, the CPIZ exhibited the highest peak concentrations for most hazardous elements, including Cd, As, Cu, Pb, and Ni (Fig. 3). This pattern strongly suggests a cumulative and intensified contamination

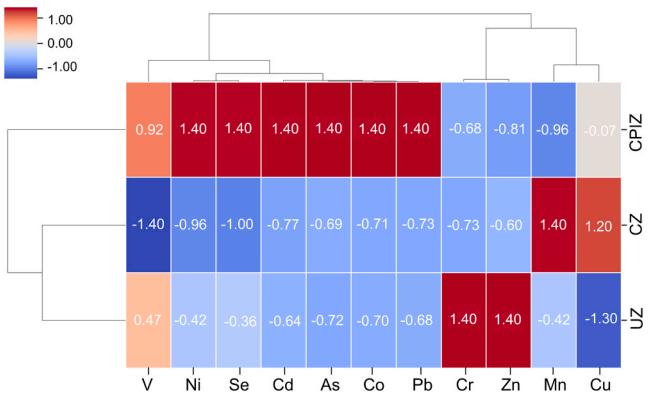

Fig. 3. Clustered heatmap of standardized maximum metal(loid) concentrations across three zones: CPIZ (coastal petrochemical industrial zone), CZ (countryside zone), and UZ (urban zone).

likely driven by industrial emissions, petrochemical processes, and potential atmospheric deposition [4,40,41]. While food preparation-related contamination cannot be entirely excluded, the alignment of contamination patterns with local land-use and industrial activity supports the conclusion that environmental sources, rather than kitchen utensils or cooking methods, are the dominant contributors to the observed metal(loid) levels.

In contrast, the CZ showed elevated maximum values of Mn and Zn, which are essential elements but may indicate over-application of agrochemicals or geogenic enrichment in local soils (Fig. 3). The UZ displayed notably high maximum concentrations of Cr, Se, and Zn in certain samples, which may stem from mixed sources such as traffic-related emissions, domestic wastewater, or market food handling practices.

The hierarchical clustering grouped CPIZ separately from CZ and UZ, reinforcing the unique and more hazardous contamination profile of the industrial zone. Moreover, Cd, As, and Pb clustered tightly together, implying possible co-contamination pathways and shared sources in CPIZ (Fig. 3). This pattern reveals the necessity of zone-specific contamination source tracking and the urgent need for risk management in food safety surveillance systems, especially in industrial coastal regions where multiple pollutants may co-occur at harmful levels. Future studies could further refine exposure assessments by incorporating standardized food categories and controlled cooking processes to isolate environmental contributions more precisely.

3.3. Human health risk in three different zones

The target hazard quotient (THQ), total target hazard quotient (TTHQ), and carcinogenic risk (CR) values across the three zones in the Caofeidian District are presented in Fig. 4 and Table S4. Among these zones, CZ exhibited the highest average TTHQ, followed by UZ and CPIZ. Notably, the TTHQ values of all food samples from the three zones exceeded the threshold value of 1.0, indicating a significant non-carcinogenic health risk associated with the long-term consumption of any single aquatic food item. An examination of the contribution of individual metal(loid)s to the total non-carcinogenic risk revealed that arsenic (As), cadmium (Cd), cobalt (Co), and copper (Cu) were the primary contributors, accounting for average percentages of 33.79 %, 24.54 %, 9.56 %, and 9.09 %, respectively, across CPIZ, CZ, and UZ. This suggests that elevated TTHQ values were largely driven by these four elements, which should be prioritized in future pollution mitigation and dietary exposure risk management.

In terms of carcinogenic risk, all food samples from CPIZ exceeded the commonly accepted threshold of 1.0×10^{-4}, indicating a potential unacceptable lifetime cancer risk. The majority of samples from CZ and UZ also surpassed this threshold, highlighting concerns over long-term carcinogenic effects due to chronic dietary exposure.

Despite these findings, THQ (V) remained below 1.0 for most food items in CPIZ and for all items in CZ and UZ, suggesting negligible non-carcinogenic risk from this element. Similarly, THQ values for Cr and Pb were consistently below 1.0 across all zones, indicating limited health risks. Comparable trends were observed for most food items with respect to Mn, Co, Cu, Zn, As, Se, Cd, and Ni, where THQ values remained below the risk threshold in the majority of cases. It should be noted that food items varied across the three zones due to differences in local dietary patterns and ingredient availability. This food diversity inherently contributed to variations in metal(loid) exposure pathways and risk levels. Nevertheless, all samples were based on actual consumed meals prepared with locally sourced ingredients, ensuring realistic assessment of zone-specific dietary risks. While the lack of uniform food items across zones prevents direct dish-to-dish risk comparison, the study aimed to assess the overall health risks within each representative dietary context. The potential influence of cooking utensils or spices was minimized through large sample sizes and randomized sampling procedures, reducing systematic bias.

It is important to recognize that while these risk assessments suggest potential health concerns, the models employed are inherently conservative and may overestimate actual human exposure. Factors such as the bioavailability of metal(loid)s, regional dietary variations, and common food preparation methods (e.g., washing, peeling, or cooking) are not fully incorporated into the calculations. Moreover, the human body possesses intrinsic detoxification and metabolic mechanisms that can reduce the effective internal dose of contaminants, and individual susceptibility can vary with age, health status, and nutritional condition. Therefore, the estimated risks should be interpreted in the context of local dietary habits and food sourcing practices, with awareness that food composition differences reflect real-world exposure patterns within each zone.

Consequently, although the results point to potential health risks—particularly with prolonged exposure—they do not necessarily imply immediate adverse outcomes. These findings underscore the necessity for ongoing environmental surveillance, stricter control of key contaminants (especially As and Cd), and the formulation of science-based public health advisories. Future studies should aim to incorporate bioaccessibility assessments and cooking loss factors to refine exposure estimates. Additionally, efforts to standardize sampled food categories and control cooking variables could further improve the precision of future risk assessments. Meanwhile, risk communication should be conducted in a balanced and evidence-informed manner to foster public awareness without inciting undue concern, while promoting safe and sustainable consumption of aquatic products.

3.4. Influence of the CPIZ on regional metal(loid) distribution

The results of the LLE analysis demonstrated that 100 % of the original data variance was effectively retained, with LLE1 and LLE2 each accounting for 50 % of the total information (Fig. 5A), indicating the strong data-reduction capability of the LLE technique. When the samples from the three zones were projected onto the LLE1–LLE2 space, a certain degree of spatial overlap between samples from the coastal petrochemical industrial zone and those from both the countryside and urban zones was observed (Fig. 5A). This overlap occurred despite clear differences in food items and cooking styles across zones, suggesting that industrial emissions in the CPIZ could influence metal(loid) accumulation in locally sourced ingredients used across all zones, rather than being strictly linked to specific dishes or cooking methods. This suggests that the influence of industrial activities in the coastal zone may have extended to surrounding regions, potentially affecting food items consumed by residents in non-industrial areas.

To further elucidate the contribution of individual elements to the observed spatial patterns, Random Forest regression was applied. For LLE1, Zn, Se, and Pb were identified as the most influential variables,

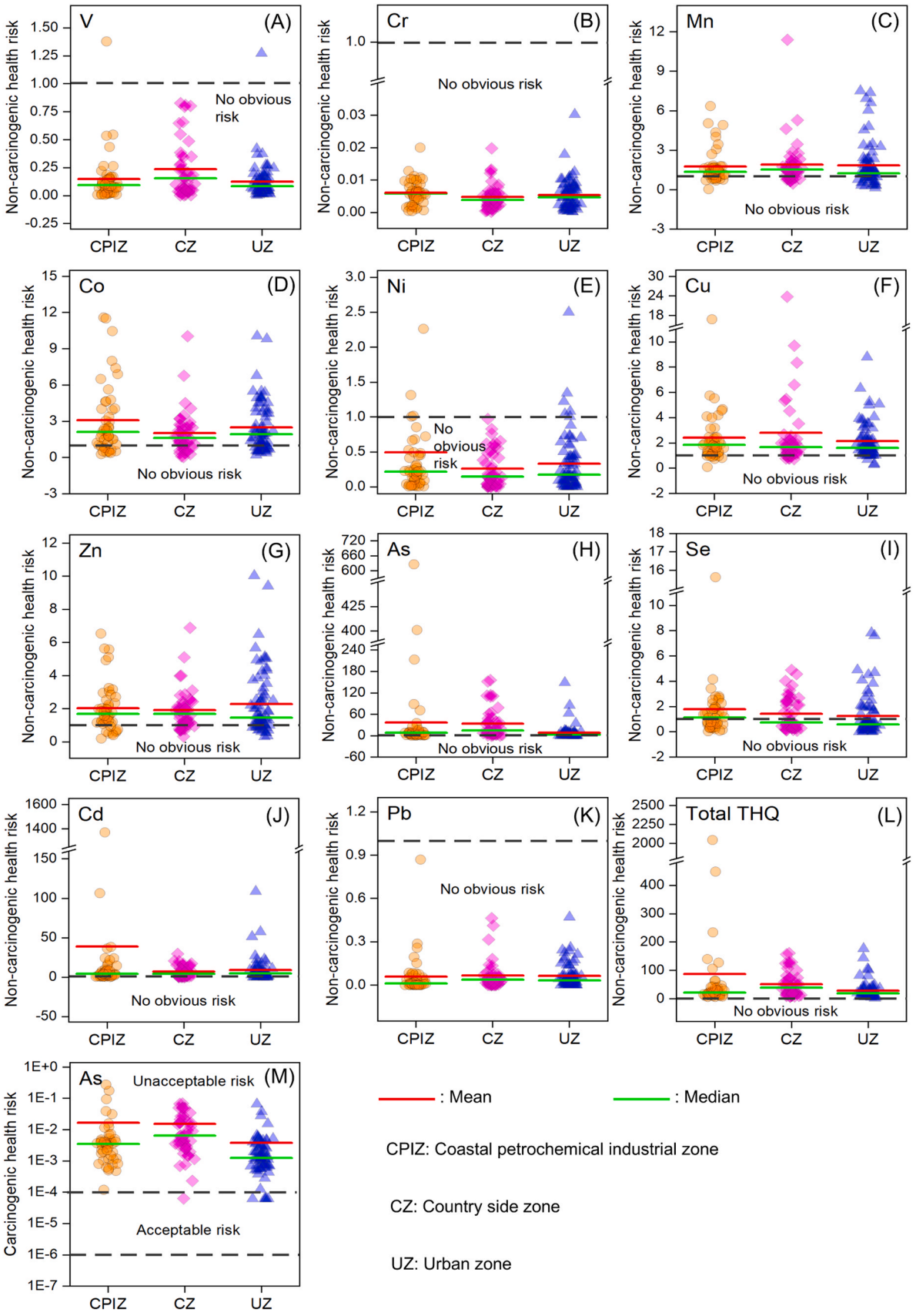

Fig. 4. Target hazard quotients (THQs) for individual metal(loid)s (A–K), total target hazard quotient (TTHQ) (L), and carcinogenic risk (CR) (M) associated with the consumption of food items collected from three zones in the Caofeidian District, Tangshan City, China.

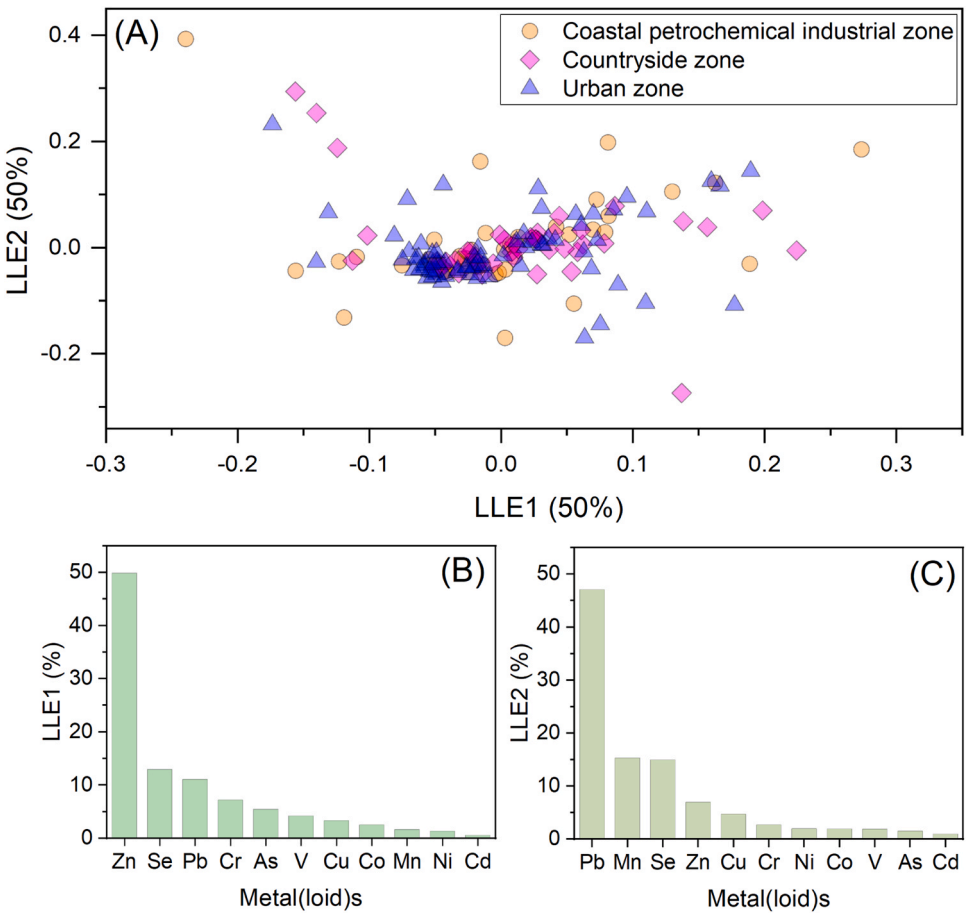

Fig. 5. Sample distribution and metal(loid) contributions based on LLE and Random Forest regression analysis. (A) Mapping of sample distribution on LLE1 and LLE2. The plot shows the distribution of samples from the coastal petrochemical industrial zone, countryside zone, and urban zone in the LLE1 and LLE2 space. The samples from the coastal petrochemical industrial zone overlap with those from the countryside zone and urban zone, indicating the influence of industrial activities on food items consumed in surrounding areas. (B) Contribution of metal(loid)s to LLE1 based on Random Forest regression analysis. This plot illustrates the relative contributions of different metal(loid)s to LLE1, with Zn, Se, and Pb being the most significant contributors. (C) Contribution of metal(loid)s to LLE2 based on Random Forest regression analysis. This plot presents the contributions of metal(loid)s to LLE2, with Pb, Mn, and Se showing the largest contributions.

contributing 49.87 %, 12.94 %, and 11.06 %, respectively, while the remaining eight elements each contributed less than 7.20 % (Fig. 5B). For LLE2, Pb, Mn, and Se contributed 47.08 %, 15.32 %, and 14.98 %, respectively (Fig. 5C). These findings indicate that Zn, Se, Pb, and Mn are the primary drivers of inter-zone differences and likely represent the key metal(loid)s through which the coastal petrochemical industrial zone exerts environmental influence.

The identification of Zn, Se, Pb, and Mn as key contributors highlights the pervasive and far-reaching impact of industrial emissions from the coastal petrochemical industrial zone. Such areas are typically associated with high-intensity industrial processes and emissions, which can lead to the accumulation of pollutants in local environmental matrices and subsequent transfer through the food web. Zn and Pb, in particular, are well-documented for their environmental persistence and bioaccumulation potential, making them pollutants of significant concern. The high contribution of Zn (49.87 %) suggests it plays a dominant role in shaping exposure patterns in adjacent regions. While Zn is an essential micronutrient, elevated levels can be toxic, potentially causing gastrointestinal distress and neurological impairment.

Se also emerged as a significant contributor in both LLE1 and LLE2 analyses. Although Se is essential in trace amounts, excessive exposure can lead to selenosis, which negatively impacts the nervous system and various internal organs. The elevated presence of Se in the coastal zone may be attributed to its release from industrial processes such as petroleum refining and coal combustion.

Pb, a toxic heavy metal with no known biological function, remains a serious public health threat. Its substantial contribution across both LLE dimensions underscores the persistence of lead contamination despite existing regulatory measures. This reveals the need for continued monitoring and intervention in regions adjacent to industrial sources. Similarly, Mn, which can be neurotoxic at high concentrations, was another key contributor in the coastal zone. Industrial emissions are a known source of Mn contamination, and its elevated levels in food products suggest a potential risk for local populations, especially those reliant on locally sourced produce and aquatic foods. Importantly, the spatial clustering results suggest that regional contamination patterns are more strongly linked to the origin of raw food materials (e.g., seafood, vegetables, grains) rather than specific cooking utensils or recipes. Given that cookware and spices are highly variable at the household and restaurant level, their potential influence would have resulted in more random spatial patterns, which was not observed. Instead, the consistent identification of Zn, Se, Pb, and Mn as zone-specific contributors implies environmental rather than culinary sources. While potential contamination from cooking utensils or condiments cannot be entirely ruled out, the diversity of food sources (including households, canteens, and restaurants) and the observed spatial differences suggest that such contamination is unlikely to be systematic. Nonetheless, the absence of utensil and condiment blank controls represents a limitation of the present study, which should be addressed in future research.

Overall, these findings indicate the interconnectedness of industrial

activity, environmental contamination, and food safety. The spatial overlap observed between industrial and non-industrial zones further emphasizes the transboundary nature of pollution and the need for regional-scale environmental management strategies. Future research should include longitudinal monitoring to assess temporal changes in contamination levels and associated health risks. Additionally, expanding the analytical scope to include a broader range of pollutants and environmental factors would provide a more comprehensive understanding of contamination dynamics and their implications for public health.

3.5. Study limitations

Several limitations of this study should be acknowledged. First, food samples were collected using the duplicate diet method to reflect real-world dietary exposure patterns. However, differences in food categories across zones, driven by local dietary habits, may have introduced variability in measured metal(loid) concentrations due to differing accumulation capacities among food types. Therefore, the comparison across zones reflects combined effects of environmental contamination and regional dietary structures, rather than standardized food items.

Second, while efforts were made to ensure that all ingredients were locally sourced within each zone, absolute confirmation of 100 % local origin was not possible in all cases, especially for certain seasonally unavailable or widely distributed products. This may have introduced minor uncertainties regarding the precise geographic origin of some raw ingredients.

Third, potential contamination from cooking utensils, cookware, or condiments cannot be entirely ruled out, as blank controls for kitchenware and spices were not included in the study design. Although food samples were collected from diverse sources, including households, canteens, and restaurants, and contamination patterns displayed clear spatial clustering consistent with local environmental conditions, the absence of utensil and spice controls represents a limitation that should be addressed in future investigations.

Finally, the use of total metal(loid) concentrations without incorporating bioaccessibility or cooking loss factors may have led to overestimations of dietary exposure and health risks. Individual variation in consumption habits, metabolic capacity, and detoxification mechanisms were also not accounted for in the risk assessment models, potentially affecting the precision of health risk predictions.

Taken together, these limitations suggest that while the study provides valuable insight into regional dietary exposure to metal(loid)s in coastal industrial areas, results should be interpreted with caution. Future research should aim to adopt standardized food categories, incorporate utensil/spice blanks, trace ingredient sourcing more precisely, and include bioaccessibility analyses to refine exposure assessments.

4. Conclusion

This study demonstrated that coastal petrochemical industrial zones exerted a measurable influence on foodborne metal(loid) contamination in nearby countryside and urban areas. By integrating the Double-Meal Method with Locally Linear Embedding and Random Forest regression, Zn, Se, Pb, and Mn were identified as the primary contributors to spatial variation across zones. The results provide compelling evidence that industrial emissions extend beyond the coastal zone, affecting food safety and posing potential health risks to adjacent populations. These findings underscore the importance of region-specific environmental surveillance and targeted pollution control strategies to mitigate human exposure risks.

Environmental implication

This study reveals the critical link between industrial contamination and foodborne exposure, revealing how pollutants from coastal petrochemical zones extend to nearby rural and urban zones. By identifying key metal(loid)s in food items, it demonstrates the need for targeted pollution control strategies. The findings contribute to understanding the transboundary nature of industrial pollution, offering valuable insights for ecosystem protection and sustainable regional planning. These results are essential for shaping policies aimed at reducing environmental and public health risks in areas affected by industrial activities.

CRediT authorship contribution statement

Yanpeng Gao: Writing – original draft, Visualization, Validation, Supervision, Software, Resources, Project administration, Methodology, Investigation, Funding acquisition, Formal analysis, Data curation. **Richard W. Jordan:** Writing – review & editing, Validation, Data curation. **Shixing Ren:** Validation, Data curation. **Kai Huang:** Methodology, Investigation. **Weng Weixin:** Validation, Methodology, Investigation, Data curation. **Shi-Jun Jiang:** Writing – review & editing, Validation, Data curation. **Yang-Guang Gu:** Writing – review & editing, Validation, Supervision, Resources, Formal analysis, Data curation, Conceptualization. **Yuemeng Ji:** Validation, Investigation, Data curation.

Declaration of Competing Interest

The authors declare that they have no known competing financial interests or personal relationships that could have appeared to influence the work reported in this paper.

Acknowledgments

We thank the National Key Research and Development Program of China (2019YFC1804501, 2022YFC3105600), National Natural Science Foundation of China (42322704, 42277222), Guangdong Basic and Applied Basic Research Foundation (2023B1515020078). As the corresponding author, this work holds particular significance for me, as it coincided with a special moment in my life—my second child was born just 60 days after the manuscript was completed. Therefore, the publication of this paper represents not only a professional achievement but also a deeply personal and memorable milestone.

Appendix A. Supporting information

Supplementary data associated with this article can be found in the online version at doi:10.1016/j.jhazmat.2025.139525.

Data availability

Data will be made available on request.

References

[1] Xu, Z.C., Chau, S.N., Chen, X.Z., Zhang, J., Li, Y.J., Dietz, T., Wang, J., Winkler, J. A., Fan, F., Huang, B.R., Li, S.X., Wu, S.H., Herzberger, A., Tang, Y., Hong, D.Q., Li, Y.K., Liu, J.G., 2020. Assessing progress towards sustainable development over space and time. Nature 577, 74–78.

[2] Gu, Y.G., Wang, Y.S., Jordan, R.W., Gao, Y.P., Huang, H.H., Jiang, S.J., 2025. Impact of coastal industrialization and urbanization on marine phosphorus cycle: insights from daya bay and zhelin bay. Gondwana Res 140, 81–88.

[3] Connor, D.S., Xie, S.Q., Jang, J., Frazier, A.E., Kedron, P., Jain, G., Yu, Y.L., Kemeny, T., 2025. Big cities fuel inequality within and across generations. PNAS Nexus 4.

[4] Gu, Y.G., Jiang, S.J., Jordan, R.W., Huang, H.H., Wu, F.X., 2023. Nonmetric multidimensional scaling and probabilistic ecological risk assessment of trace metals in surface sediments of daya bay (China) using diffusive gradients in thin films. Sci Total Environ 867, 161433.

[5] Li, C.M., Wang, H.C., Liao, X.L., Xiao, R., Liu, K.H., Bai, J.H., Li, B., He, Q., 2022. Heavy metal pollution in coastal wetlands: a systematic review of studies globally over the past three decades. J Hazard Mater 424, 127312.

[6] Gu, Y.G., Gao, Y.P., Chen, F., Huang, H.H., Yu, S.H., Jordan, R.W., Jiang, S.J., 2022. Risk assessment of heavy metal and pesticide mixtures in aquatic biota using the DGT technique in sediments. Water Res 224, 119108.
[7] Swain, C.K., 2024. Environmental pollution indices: a review on concentration of heavy metals in air, water, and soil near industrialization and urbanisation. Discov Environ 2, 5.
[8] Zarei, S., Karbassi, A., Sadrinasab, M., Sarang, A., 2023. Investigating heavy metal pollution in anzali coastal wetland sediments: a statistical approach to source identification. Mar Pollut Bull 194, 115376.
[9] Li, K., Wang, J.Y., Zhang, Y.W., 2022. Heavy metal pollution risk of cultivated land from industrial production in China: spatial pattern and its enlightenment. Sci Total Environ 828, 154382.
[10] Song, B., Lei, M., Chen, T.B., Zheng, Y.M., Xie, Y.F., Li, X.Y., Gao, D., 2009. Assessing the health risk of heavy metals in vegetables to the general population in Beijing, China. J Environ Sci 21, 1702–1709.
[11] Varol, M., Gündüz, K., Sünbül, M.R., Aytop, H., 2022. Arsenic and trace metal concentrations in different vegetable types and assessment of health risks from their consumption. Environ Res 206, 112252.
[12] Wei, J.X., Cen, K., 2020. Contamination and health risk assessment of heavy metals in cereals, legumes, and their products: a case study based on the dietary structure of the residents of Beijing, China. J Clean Prod 260, 121001.
[13] Huang, F.Y., Li, Z.M., Yang, X., Liu, H.J., Chen, L., Chang, N., He, H.R., Zeng, Y., Qiu, T.Y., Fang, L.C., 2024. Silicon reduces toxicity and accumulation of arsenic and cadmium in cereal crops: a meta-analysis, mechanism, and perspective study. Sci Total Environ 918, 170663.
[14] Wang, X.N., Wang, Z.H., Jiang, S.J., Jordan, R.W., Gu, Y.G., 2023. Bioenrichment preference and human risk assessment of arsenic and metals in wild marine organisms from dapeng (Mirs) bay, South China Sea. Mar Pollut Bull 194, 115305.
[15] Liu, R., Jiang, W., Li, F., Pan, Y., Wang, C., Tian, H., 2021. Occurrence, partition, and risk of seven heavy metals in sediments, seawater, and organisms from the eastern sea area of shandong peninsula, yellow sea, China. J Environ Manag 279, 111771.
[16] Wang, X.L., Zhang, Y., Geng, Z., Liu, Y., Guo, L.X., Xiao, G.X., 2019. Spatial analysis of heavy metals in meat products in China during 2015–2017. Food Control 104, 174–180.
[17] Gao, Y.P., Geng, M.Z., Wang, G.Y., Yu, H., Ji, Y.M., Jordan, R.W., Jiang, S.J., Gu, Y. G., An, T.C., 2024. Environmental and dietary exposure to 24 polycyclic aromatic hydrocarbons in a typical Chinese coking plant. Environ Pollut 346, 123684.
[18] Shim, J.-S., Oh, K., Kim, H.C., 2014. Dietary assessment methods in epidemiologic studies. Epidemiol Health 36, e2014009.
[19] Wang, T.-C., 2023. Developing a flexible and efficient dual sampling system for food quality and safety validation. Food Control 145, 109483.
[20] Keck, F., Peller, T., Alther, R., Barouillet, C., Blackman, R., Capo, E., Chonova, T., Couton, M., Fehlinger, L., Kirschner, D., Knüsel, M., Muneret, L., Oester, R., Tapolczai, K., Zhang, H., Altermatt, F., 2025. The global human impact on biodiversity. Nature.
[21] Ezzat, L., Peter, H., Bourquin, M., Busi, S.B., Michoud, G., Fodelianakis, S., Kohler, T.J., Lamy, T., Geers, A., Pramateftaki, P., Baier, F., Marasco, R., Daffonchio, D., Deluigi, N., Wilmes, P., Styllas, M., Schön, M., Tolosano, M., De Staercke, V., Battin, T.J., 2025. Diversity and biogeography of the bacterial microbiome in glacier-fed streams. Nature 637, 622–630.
[22] Roweis, S.T., Saul, L.K., 2000. Nonlinear dimensionality reduction by locally linear embedding. Science 290, 2323–2326.
[23] G.E. Quaye, Random Forest For High-Dimensional Data, in, The University of Texas at El Paso, 2024.
[24] Yu, F.B., Wei, C.H., Deng, P., Peng, T., Hu, X.G., 2021. Deep exploration of random forest model boosts the interpretability of machine learning studies of complicated immune responses and lung burden of nanoparticles. Sci Adv 7, eabf4130.
[25] Breiman, L., 2001. Random forests. Mach Learn 45, 5–32.
[26] Svetnik, V., Liaw, A., Tong, C., Culberson, J.C., Sheridan, R.P., Feuston, B.P., 2003. Random forest: a classification and regression tool for compound classification and QSAR modeling. J Chem Inf Comput Sci 43, 1947–1958.
[27] Wang, Z.X., Gu, X., Ouyang, W., Lin, C.Y., Zhu, J., Xu, L., Liu, X., He, M.C., Wang, B.D., 2020. Trophodynamics of arsenic for different species in coastal regions of the northwest Pacific Ocean: in situ evidence and a meta-analysis. Water Res 184, 116186.
[28] Wang, X.N., Wang, Z.H., Jiang, S.J., Jordan, R.W., Gu, Y.G., 2023. Bioenrichment preference and human risk assessment of arsenic and metals in wild marine organisms from dapeng (Mirs) bay, South China Sea. Mar Pollut Bull 194, 115305.
[29] United States Environmental Protection Agency, Regional Screening Levels (RSLs) - Generic Tables, in, 2022. ⟨https://www.epa.gov/risk/regional-screening-levels-rsls-generic-tables⟩.
[30] D. Han, Y.H. Zhang, Forging Ahead for 75 Years: Tangshan Steps into a New Era, in, 2024.
[31] Tangshan Municipal Bureau of Statistics and Tangshan Survey Team of the National Bureau of Statistics of China, Tangshan Statistical Yearbook 2023, in, 2024, pp. 374. ⟨https://www.tangshan.gov.cn/zhuzhan/tjnj/20240119/1586152.html⟩.
[32] XN, More Than 50% of Chinese Adults Now Overweight or Obese, in, 2020.
[33] WHO, Safety evaluation of certain food additives and contaminants: prepared by the seventy-third meeting of the Joint FAO/WHO Expert Committee on Food Additives, in, 2011. ⟨https://www.who.int/publications/i/item/9789241660648⟩.
[34] US E.P.A., Integrated Risk Information System, in, 2025. ⟨https://www.epa.gov/iris⟩.
[35] Kumpulainen, J.T., 1992. Chromium content of foods and diets. Biol Trace Elem Res 32, 9–18.
[36] Vincent, J.B., 2013. Chromium: is it essential, pharmacologically relevant, or toxic? In: Sigel, A., Sigel, H., Sigel, R.K.O. (Eds.), Interrelations between Essential Metal Ions and Human Diseases. Springer Netherlands, Dordrecht, pp. 171–198.
[37] Zhang, W., Wang, W.X., 2012. Large-scale spatial and interspecies differences in trace elements and stable isotopes in marine wild fish from Chinese waters. J Hazard Mater 215-216, 65–74.
[38] Li, J.G., Wu, Q.L., Hu, H.L., Ni, F.C., Ni, H.Q., Cai, X.L., 2024. Determination and health risk assessment of heavy metal content in vegetables around quarries in Southern fujian province. Chin J Trop Agric 44, 79–83.
[39] Bi, C.J., Zhou, Y., Chen, Z.L., Jia, J.P., Bao, X.Y., 2018. Heavy metals and lead isotopes in soils, road dust and leafy vegetables and health risks via vegetable consumption in the industrial areas of shanghai, China. Sci Total Environ 619-620, 1349–1357.
[40] Gu, Y.G., Wang, X.N., Lin, Q., Du, F.Y., Ning, J.J., Wang, L.G., Li, Y.F., 2016. Fuzzy comprehensive assessment of heavy metals and pb isotopic signature in surface sediments from a bay under serious anthropogenic influences: daya bay, China. Ecotoxicol Environ Saf 126, 38–44.
[41] Gu, Y.G., Wang, Z.H., Lu, S.H., Jiang, S.J., Mu, D.H., Shu, Y.H., 2012. Multivariate statistical and GIS-based approach to identify source of anthropogenic impacts on metallic elements in sediments from the mid guangdong coasts, China. Environ Pollut 163, 248–255.